ISBN: 978-981-94-1156-6
2024 the 14th International Workshop on Computer Science and Engineering (WCSE 2024)
doi: 10.18178/wcse.2024.06.035

A Method for Extracting Weak Heartbeat Signal from Radar Echo Signal

Zhen Li [1, a1+], Zhen Ruan [1,b], Lei Zhang [1,c], Xi Liu [1,d], Hongliang Chen [1,e], Ziyou Wang [1,f]

[1]Shanghai Fire Science and Technology Research Institute of MEM, Shanghai, China

[a]324720808@qq.com, [b]ruanzhen@shfri.cn, [c]zhanglei@shfri.cn, [d]866524798@qq.com, [e]chenhongliang@shfri.cn, [f]wangziyou@shfri.cn

Abstract. The article proposes a method that combines complete ensemble empirical mode decomposition with adaptive noise (CEEMDAN) and multiple autocorrelations to address the issue of weak center-beat signals in radar echo signals, which are prone to being obscured by strong clutter, thus preventing the extraction of valid data. The respiratory and heartbeat signals are distinguished based on the energy distribution of different frequency bands in various intrinsic mode functions (IMFs). Subsequently, different thresholds are applied to filter the respiratory and heartbeat signals separately. Principal components are selected using the principal component analysis (PCA) algorithm, and their signal-to-noise ratio is further enhanced through multiple autocorrelations. Finally, the respiratory and heartbeat signals are reconstructed by cross-correlating the real and imaginary components. Simulation results demonstrate the effectiveness of the proposed method in extracting weak heartbeat signals and obtaining satisfactory measurement data outcomes.

Keywords: ensemble empirical mode decomposition with adaptive noise, multiple autocorrelations, low signal-to-noise ratio, principal component analysis.

1. Introduction

Non-contact monitoring methods can reduce discomfort for the monitored subjects and avoid issues caused by the detachment of contact devices, in comparison to traditional contact monitoring methods. Bio-radar, which utilizes electromagnetic waves to emit and receive signals, can obtain physiological information of living organisms. This technology has extensive applications in fields such as military medicine, disaster medicine, and urban anti-terrorism.

Life characteristic signals consist of parameters including respiration and heartbeat, which are typically very weak and easily overshadowed by strong interference. Accurately extracting life characteristic signals from strong interference is the key focus of this study. Data analysis reveals that life signals have low signal-to-noise ratios and exhibit characteristics of low frequency, quasi-periodicity, and harmonics, while interference signals can be approximated as Gaussian colored noise. Therefore, the signal processing of bio-radar can be simplified as the extraction of signals from a harmonic model distorted by Gaussian colored noise and improving signal-to-noise ratio.

Firstly, the received signals are decomposed into modal components with different frequency characteristics using complete ensemble empirical mode decomposition with adaptive noise CEEMDAN [5]. The energy of each modal component within the frequency range of 0.05Hz-0.8Hz and 0.8Hz-3.0Hz is

+ Corresponding author. Tel.: +8613817610068; fax: +86 021 64160597.
E-mail address: 324720808@qq.com.

computed, and adaptive thresholds are applied to select respiratory and heartbeat signals. Secondly, principal component analysis (PCA) is utilized to further refine the selected heartbeat signals, ultimately improving the signal-to-noise ratio. Lastly, the final heartbeat signals are obtained through multiple autocorrelations.

2. Signal Model

Respiratory and heartbeat signals cause very small movements in the chest wall, which can be expressed as a series of simple harmonic motion about time. The instantaneous distance from the antenna to the chest wall is given by

$$\Delta r(t) = r_0 + \Delta_1 \sin(2\pi f_1 t) + \Delta_2 \sin(2\pi f_2 t) \tag{1}$$

where r_0 is the distance from the chest cavity to the center of the receiving antenna, Δ_1, Δ_2, f_1 and f_2 are the amplitudes and frequencies of respiratory signal and heartbeat signal.

$$\Delta\varphi = \frac{4\pi}{\lambda}\Delta r(t) \tag{2}$$

According to the aforementioned analysis and modeling simulation, a Gaussian noise with a signal-to-noise ratio of 10 dB was added to the radar echo signal simulated in MATLAB, as shown in the figure below.

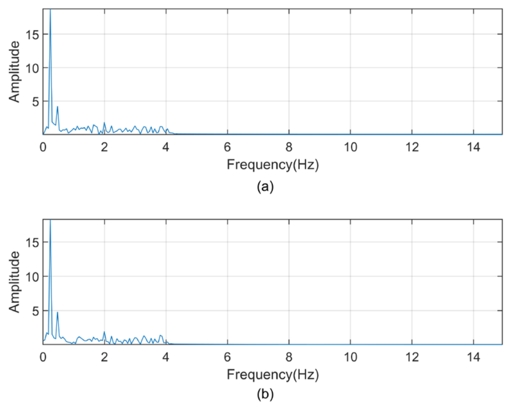

Fig. 1: The frequency-domain echo signal. (a) Not filtered through a low-pass filter. (b) Filtered through a low-pass filter.

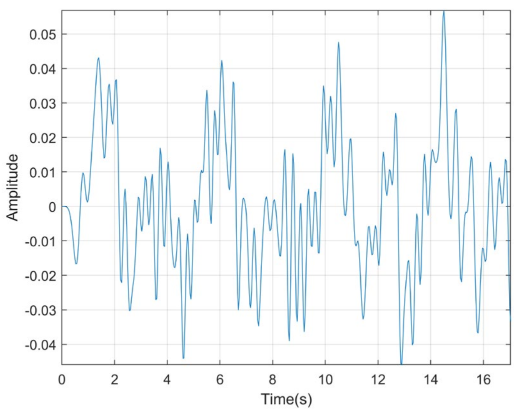

Fig. 2: The time-domain echo signal.

In Fig. 1(a), the radar echo signal in the frequency domain is shown with original noise. Fig. 1(b) illustrates the radar echo signal processed by a low-pass digital filter with a cutoff frequency of 0 Hz-4 Hz. The

$f_1 = 0.23438$ Hz corresponds to the respiratory signal, while the $f_2 = 0.99609$ Hz, which is nearly submerged, represents the heartbeat signal. Both signals have been corrupted with 10 dB of noise. Fig. 2 presents the time-domain analysis of the radar echo signal, and the subsequent section will delve into the denoising analysis process.

3. Signal Processing

3.1. Signal Decomposition

Given that both the respiratory and heartbeat signals exist within the echo signal, it can be challenging to denoise the signals without accidentally removing the smaller signal (heartbeat) as noise from the larger signal (respiration). Therefore, separating the respiratory and heartbeat signals is necessary. To achieve this, CEEMDAN can decompose the original signal into multiple Intrinsic Mode Function (IMF) components based on the signal peaks and their corresponding frequency points. This decomposition facilitates the separation of the two distinct signals.

The CEEMDAN [1] [7] algorithm is an improved version of the empirical mode decomposition (EMD) algorithm. It introduces the addition of a finite number of adaptive white noise components to address the issue of mode mixing in EMD. In the CEEMDAN algorithm, the decomposed components obtained from the decomposition are denoted as I_{IMF_1}. Here, the calculation method for I_{IMF_1} is the same as the one used to compute I_{IMF_1} in the EEMD algorithm. The operator $E_j(\cdot)$ represents the j-th mode component sequence obtained through the EMD algorithm. ω_i is the Gaussian white noise adhering to $N(0,1)$ added during the i-th iteration. Assuming $f(t)$ as the original signal sequence to be processed, after adding white noise, it becomes $f(t) = \varepsilon_0 \omega_i(t)$. The CEEMDAN algorithm is then utilized to decompose the original signal sequence with the added white noise. The process is as follows:

First, the EMD algorithm is employed to decompose and obtain the first mode component, denoted as:

$$I_{IMF_1}(t) = \frac{1}{N}\sum_{i=1}^{N} I_{IMF_1}^{i}(t) \tag{3}$$

Next, the first residual signal, denoted as $R_1(t) = f(t) - I_{IMF_1}(t)$, is calculated. The signal $R_1(t) + \varepsilon_1 E_1 \omega_i(t)$ is repeatedly decomposed N times using the EMD algorithm to obtain the second mode component, denoted as:

$$I_{IMF_2}(t) = \frac{1}{N}\sum_{i=1}^{N} E_1 \cdot (R_1(t) + \varepsilon_1 E_1[\omega_i(t)]) \tag{4}$$

for $k = 2,3,...,K$, the k-th residual signal, denoted as $R_k(t) = R_{k-1}(t) - I_{IMF_k}(t)$, is calculated. The original sequence is repeatedly decomposed using the EMD algorithm to compute the ($k+1$)-th mode component.

$$I_{IMF_{(k+1)}}(t) = \frac{1}{N}\sum_{i=1}^{N} E_1 (R_1(t) + \varepsilon_k E_k[\omega_i(t)]) \tag{5}$$

The process is repeated multiple times until the residual signal is no longer suitable for further decomposition, indicating the end of the decomposition. The final residual signal is:

$$R(t) = f(t) - \sum_{i=1}^{K} I_{IMF_k}(t) \tag{6}$$

Finally, the original signal is decomposed into K mode components:

$$f(t) = R(t) + \sum_{i=1}^{K} I_{IMF_k}(t) \tag{7}$$

Fig 3 shows the Fast Fourier Transform (FFT) image of the echo signal. It can be observed that CEEMDAN decomposes the initial signal into seven Intrinsic Mode Function (IMF) components based on different frequency bands. In the low-frequency range (IMF5 ~ IMF7), the IMF components exhibit a single prominent peak. However, in the high-frequency range, there are still multiple frequency points with high energy. To address this issue, we employ energy feature analysis to achieve noise reduction.

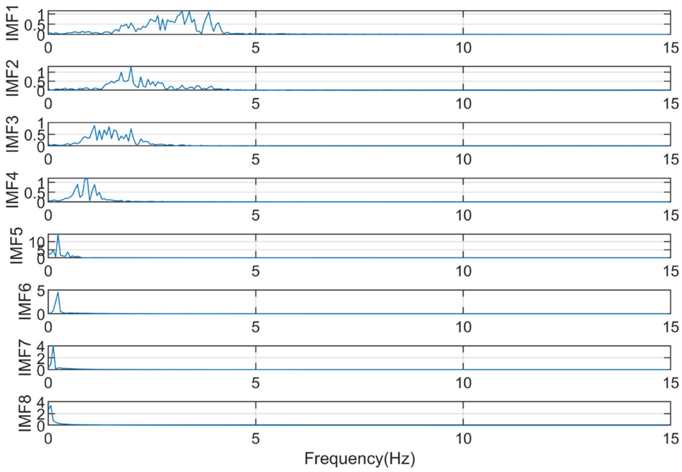

Fig.3: Figure showing the frequency-domain decomposition using CEEMDAN.

3.2. Energy Characteristic Analysis

The target signal is decomposed into a set of IMF components through the use of the CEEMDAN method.The antenna rotation Doppler is modeled and compensated by using data shifting method in the processor[10]. Each component exhibits a corresponding central frequency in its spectrum, representing either the target frequency or noise frequency. Extracting the features of the target signal from a spectral analysis perspective is challenging, as the target information is unknown. The energy spectra of each IMF component of the signal can effectively display the energy variations of different target IMF components. In this study, a feature extraction method based on the ratio of IMF energies is proposed [6].

(1) The original signal is decomposed into M IMF components using the CEEMDAN method.

(2) The energy E of each IMF component is calculated E_i.

$$E_i = \int |c_i(t)|^2 \, dt \quad i = 1, 2, ..., M \tag{8}$$

consequently, the IMF energy vector $V_E = [E_1, E_2, ..., E_M]$ is obtained.

(3) The energy vector is normalized to obtain the following equation:

$$V_E^{'} = [p_1, p_2, ..., p_M] \tag{9}$$

here, $p_i = \frac{E_i}{E}$ represents the normalization weight of each IMF component, and $E = (\sum_{i=1}^{M} E_i^2)^{\frac{1}{2}}$ represents the sum of energy for each IMF component. This calculation method allows components with higher energy proportions to receive greater weights, while components with lower energy proportions will only receive smaller weights. This is advantageous for highlighting the main components of the signal and reducing the impact of bandwidth on IMF energy analysis.

The analysis of the energy difference between the high and low frequency bands of a signal reveals distinct differences in the IMF energy distribution characteristics, which are indicative of the varying vibration mechanisms of different acoustic targets. However, due to the presence of environmental or measurement system noise, the measured signal of the target radiation noise is subject to certain influences. Therefore, relying solely on the energy vector as a target feature parameter is insufficient for target recognition. Consequently, based on the characteristics of the target, the energy difference between the high and low frequency components of the target signal is defined as a signal feature parameter. By combining the analysis of the frequency band energy difference and the IMF energy vector of the target signal, target recognition and classification can be accomplished. Assuming that the target signal has been decomposed, resulting in M -order Intrinsic Mode Function (IMF) components, let us denote that the i th-order IMF comprises L sample points. For the p th point, where the instantaneous frequency is denoted as $f_{i,p}$ and the instantaneous amplitude as $A_{i,p}$, the instantaneous intensity at point p is represented as $B_{i,p} = A_{i,p}^2$. According to the typical frequency distribution characteristics of target signals, the frequency range of 50 Hz-800 Hz is defined as the low-frequency band, and the range of 800 Hz-3000 Hz is defined as the high-frequency band. Assuming the instantaneous intensity of the time-frequency sampling points in the low-frequency band is denoted as $B_{l1}, B_{l2}, ..., B_{1m}$, the total energy of the signal in the low-frequency range, denoted as P_l, can be calculated as follows:

$$P_l = 10\lg\sum_{k=1}^{m} B_{lk} \tag{10}$$

Similarly, assuming that the instantaneous intensity of the time-frequency sampling points in the high-frequency band is denoted as $B_{l1}, B_{l2}, ..., B_{\ln}$, the total energy of the signal in the high-frequency range, denoted as P_h , can be calculated as follows:

$$P_h = 10\lg\sum_{k=1}^{n} B_{hk} \tag{11}$$

Therefore, the energy difference between the high-frequency and low-frequency components of the target signal is defined as:

$$\Delta P = P_h - P_l \tag{12}$$

After performing energy feature analysis and denoising, we obtain two segments of the signal: one ranging from 0.05 Hz to 0.8 Hz and the other ranging from 0.8 Hz to 3 Hz. These two segments correspond to respiratory and heartbeat signals, respectively. Therefore, we employ principal component analysis (PCA) to further reduce noise and select the effective components.

3.3. Multiple Autocorrelation

After performing PCA, the heartbeat and respiratory signals were successfully extracted, despite the presence of significant noise. However, multiple autocorrelation analysis is undoubtedly a better choice due to its simplicity and significant denoising effect [7]. The multiple autocorrelation detection [2] is a subsequent process that builds upon single autocorrelation detection. While single autocorrelation improves the signal-to-noise ratio of the source signal, its ability to detect and extract weak signals is limited because of the marginal improvement in the signal-to-noise ratio. On the other hand, multiple autocorrelation greatly enhances the signal-to-noise ratio by repeatedly executing single autocorrelation steps, making it more suitable for subsequent signal analysis and extraction. The overall algorithm processing flow is shown in the Fig.4 below:

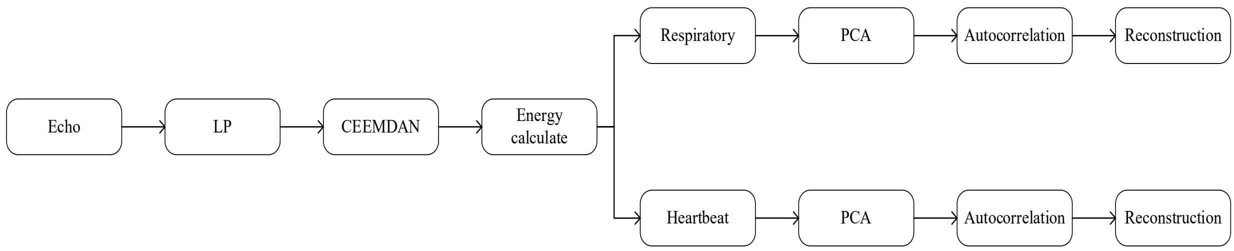

Fig. 4: Signal processing algorithm flowchart

3.4. Experimental analysis

The Fig.5 below displays the simulation results of the algorithm in this paper. The first plot shows the fixed respiratory and heartbeat frequencies, while the second plot demonstrates a fixed respiratory frequency and a variable heartbeat frequency signal. The heartbeat signal frequency was set to increase from 1Hz to 2Hz with a step size of 0.01Hz. It can be observed that after denoising, the noise is effectively eliminated. Moreover, the measured results are consistent with the set frequencies.

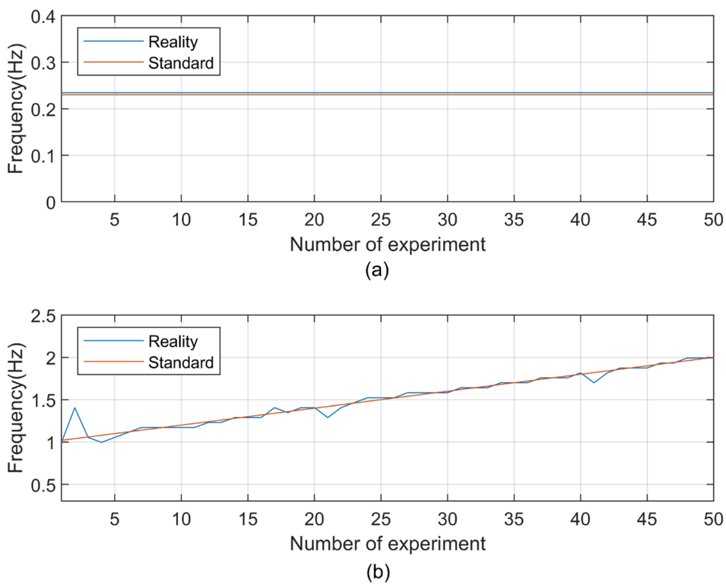

Fig. 5: Experimental data analysis results. (a) The actual values of the respiratory signals were compared to the standard values in 50 experiments. (b) The actual values of the heartbeat signals were compared to the standard values in 50 experiments.

4. Conclusion

Biological radar enables the non-contact detection of vital signs (such as breathing and body movement) and finds extensive applications in settings like homes, community hospitals, and more. However, for practical applications, it is crucial to also detect the heartbeat signal to better reflect the individual's physiological condition. Non-contact detection of respiratory signals using biological radar is relatively straightforward, as a simple digital filter with a cutoff frequency of 0.8Hz can extract the respiratory signal. On the other hand, extracting the heartbeat signal using a bandpass filter (with a lower cutoff frequency of 0.8Hz and an upper cutoff frequency of 3Hz) is challenging due to the interference of high harmonics from the respiratory signal and environmental Gaussian noise. Experimental results demonstrate that the proposed filtering method in this paper effectively separates the heartbeat signal from body movement signals. The extracted heart rate values from this signal exhibit a strong correlation with those obtained from electrocardiogram signals.

5. Acknowledgment

This paper is supported by the Project supported by the National Key Research and Development Program of China (Grant No.2021YFC3090402).

6. References

[1] Han, S., Sun, S., Cheng, Y., Wang, S., Lv, Z., Zhao, Z., & Shao, T. (2019). Short-term wind speed ensemble prediction based on improved empirical mode decomposition and support vector machine. Science, Technology and Engineering, 19(36), 172-178.

[2] Wu, L., Tian, M., & Shang, J. (2018). Research on Denoising Algorithms Based on Multiple Correlation and Adaptive Threshold. Information Technology, 42(10), 68-72.

[3] Li, S., Gao, M., & Fu, X. (2008). Signal processing and simulation of life detection radar echo. Acta Armamentarii, (06), 756-758.

[4] Zhao, H., Zhou, J., Wang, H., et al. (2018). Short-term wind speed prediction based on CEEMDAN-PE and QGA-BP. Electronic Technology Applications, 44(12), 60-64.

[5] Wei, X., Shi, Q., Fu, W., & Chen, L. (2020). Short-term wind speed prediction considering CEEMDAN sample entropy and SVR. Hydroelectric Energy Science, 38(11), 207-210.

[6] Lü, Y., Sun, S., & Gu, X. (2008). Battlefield Acoustic Target Classification and Recognition Based on EMD and Energy Ratio. Vibration and Impact, 11, 51-55, 61, 197.

[7] Chen, M., & Liu, Z. (2006). Detection of Weak Sinusoidal Signals using Multiple Autocorrelation Method. Noise and Vibration Control, 5, 28-30, 61.

[8] Qin, X., Cai, J., Liu, S., & Bian, A. (2017). Research on Denoising Method of Microseismic Signals Based on Empirical Mode Decomposition, Mutual Information Entropy, and Synchronous Compression Transform. Petroleum Exploration and Development, 56(5), 658-666.

[9] Chen, S., He, Z., Zhu, M., Wang, R., Chen, X., Wen, X., Jiang, J., & Zeng, Y. (2010). Reservoir Prediction Based on EMD and Approximate Entropy. Natural Gas Geoscience, 21(5), 828-832.

[10] Baig N A , Malik M B . Antenna rotation effects and its compensation in radar signal processing[J]. Journal of Communications, 2018, 13(9):540-545.